Electronic Supplementary Material (ESI) for Journal of Materials Chemistry A.

NbN Nanodots Decorated N-doped Graphene as Multifunctional Interlayer for High-Performance Lithium-Sulfur Batteries

Fei Ma[a#], Xiaojuan Zhang[a#], katam Srinivas[a], Dawei Liu[a], Ziheng Zhang[a], Xin Chen[a], Wanli Zhang[a], Qi Wu[b], Yuanfu Chen*[a,b]*

[a] School of Electronic Science and Engineering, and State Key Laboratory of Electronic Thin Films and Integrated Devices, University of Electronic Science and Technology of China, Chengdu 610054, PR China.

[b] College of Science and Institute of Oxygen Supply, Center of Tibetan Studies (Everest Research Institute), Tibet University, Lhasa, 850000, PR China.

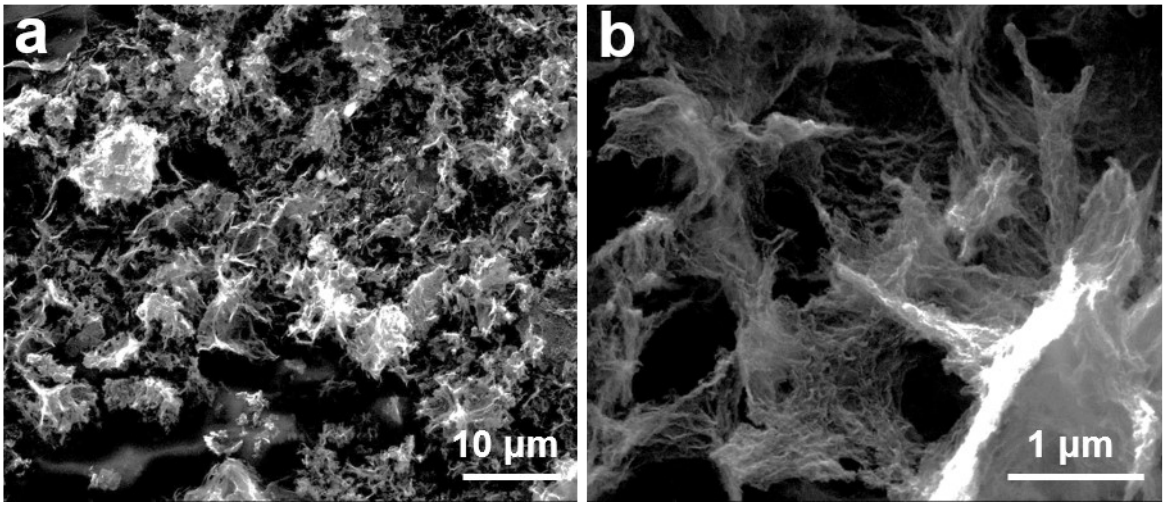

Fig. S1 FESEM image of the NG at different magnifications.

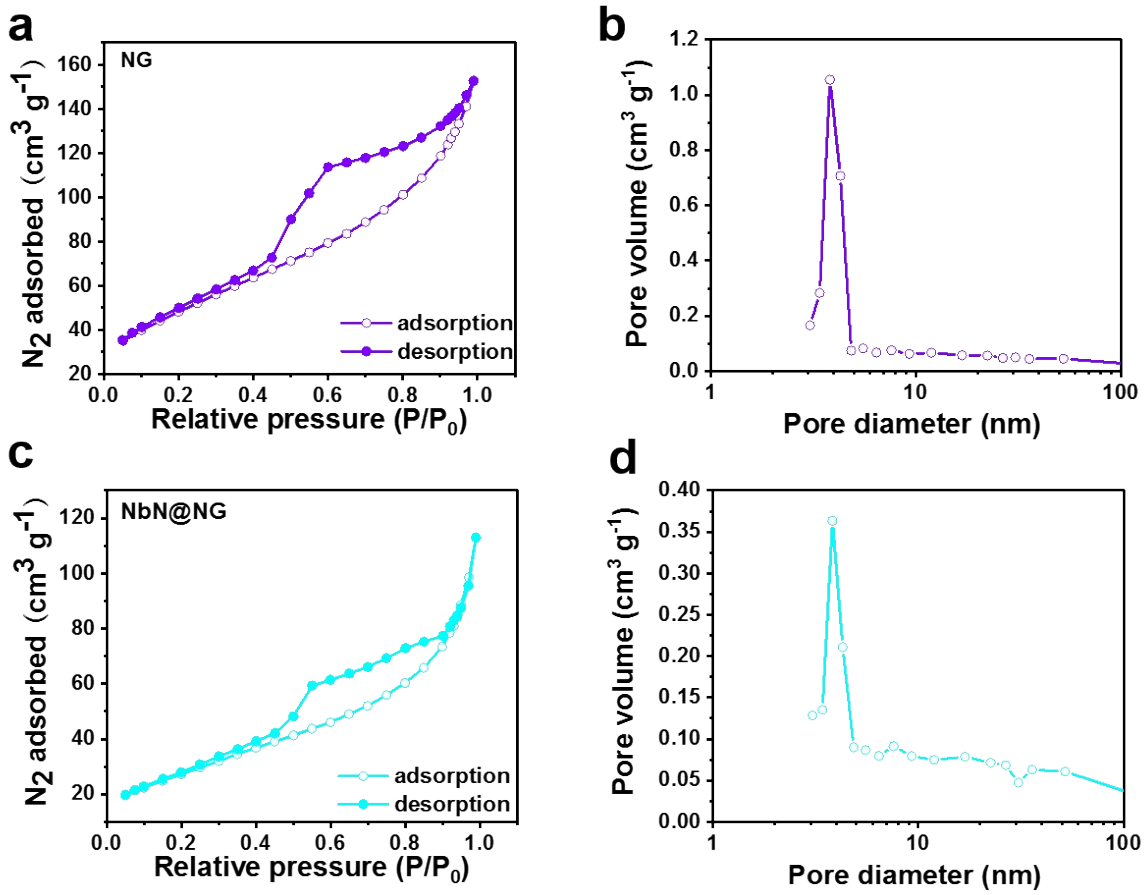

Fig. S2 N_2 adsorption and desorption isotherms of (a) NG and (b) NbN@NG. Calculated pore size distribution (c) and (d) of NG and (c) NbN@NG.

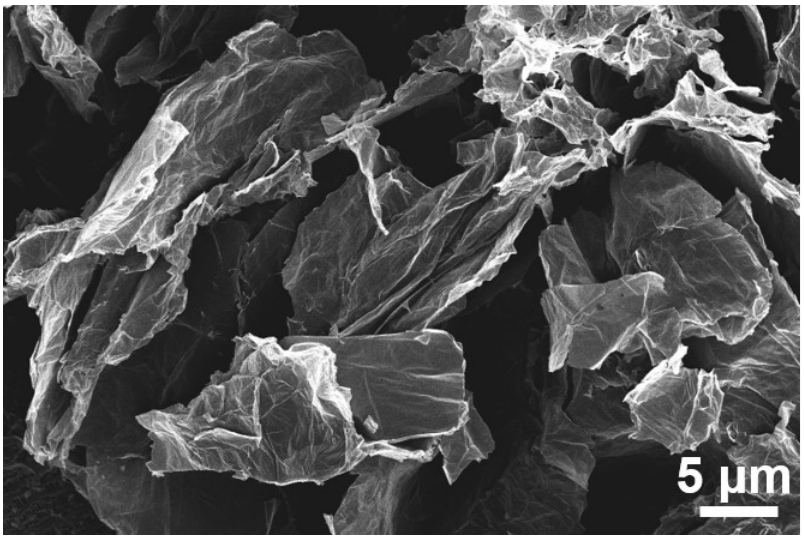

Fig. S3 SEM images of the top surface for NG modified separators.

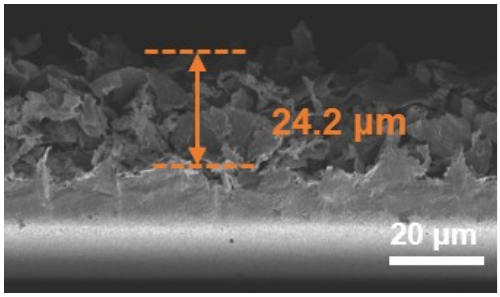

Fig. S4 Cross-section of NG modified separators.

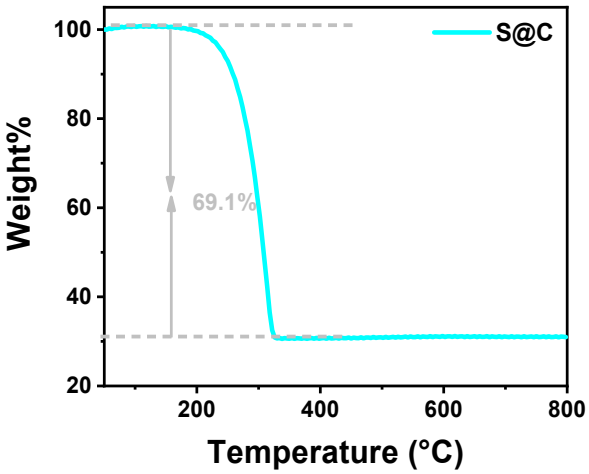

Fig. S5 TGA patterns of S@C.

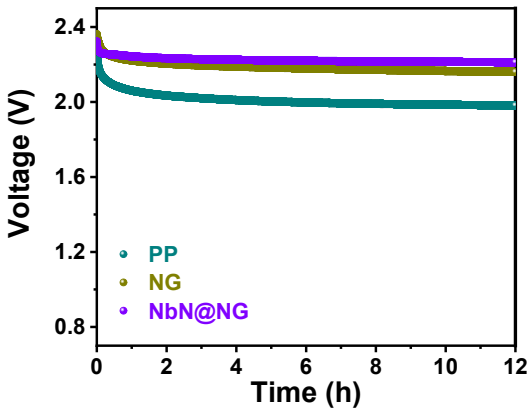

Fig. S6 Self-discharge behavior of the batteries.

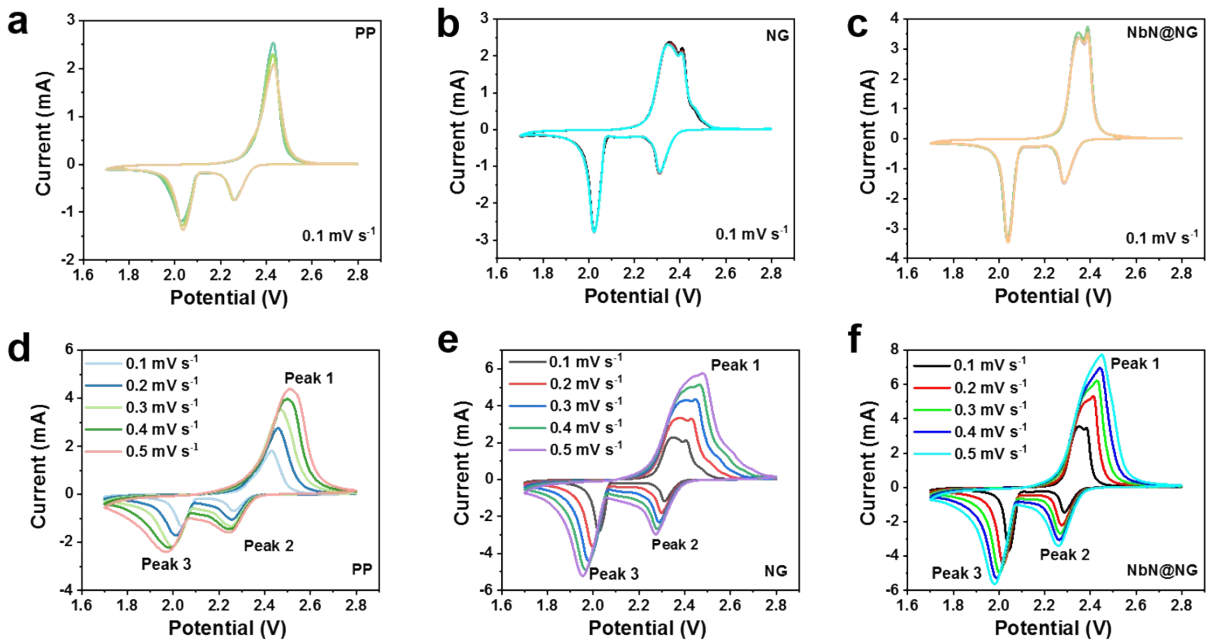

Fig. S7 CV curves of the batteries with (a) PP, (b) NG, and (c) NbN@NG separators at 0.1 mV s^{-1}. CV curves of the batteries with (d) PP, (e) NG, and (f) NbN@NG separators in the range of 0.1-0.5 mV s^{-1}.

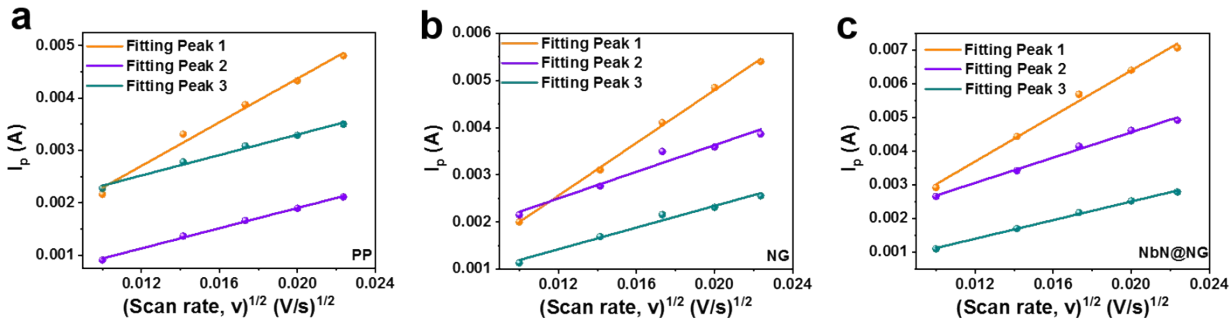

Fig. S8 (a-c) The linear fitting curves of the peak current as a function of scan rate with different separators.

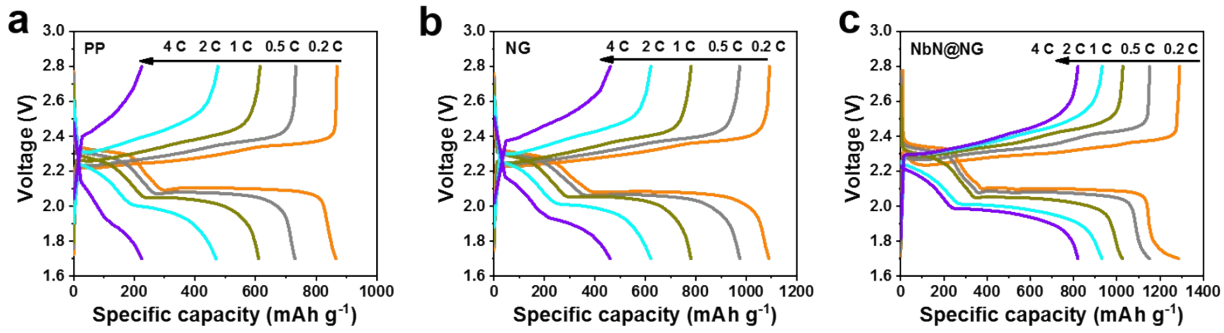

Fig. S9 Galvanostatic discharging/charging curves of the batteries with (a) PP, (b) NG, and (c) NbN@NG separator at various rates.

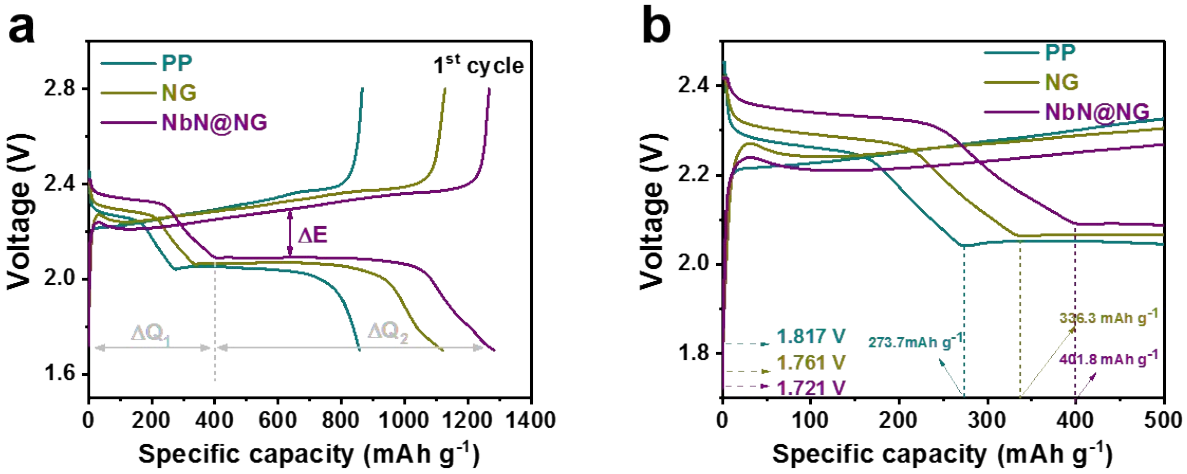

Fig. S10 (a) Galvanostatic charge/discharge curves of different separators at 0.2 C. (b) The details of charge/discharge curves.

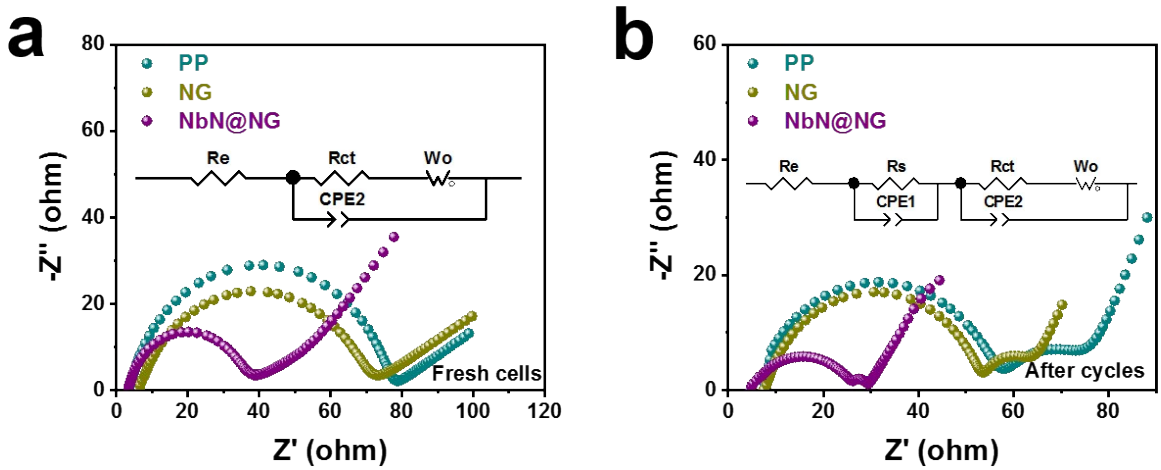

Fig. S11 Nyquist plots of the batteries with different materials (a) before and (b) after 200 cycles at 0.2 C, insets: the corresponding equivalent circuits.

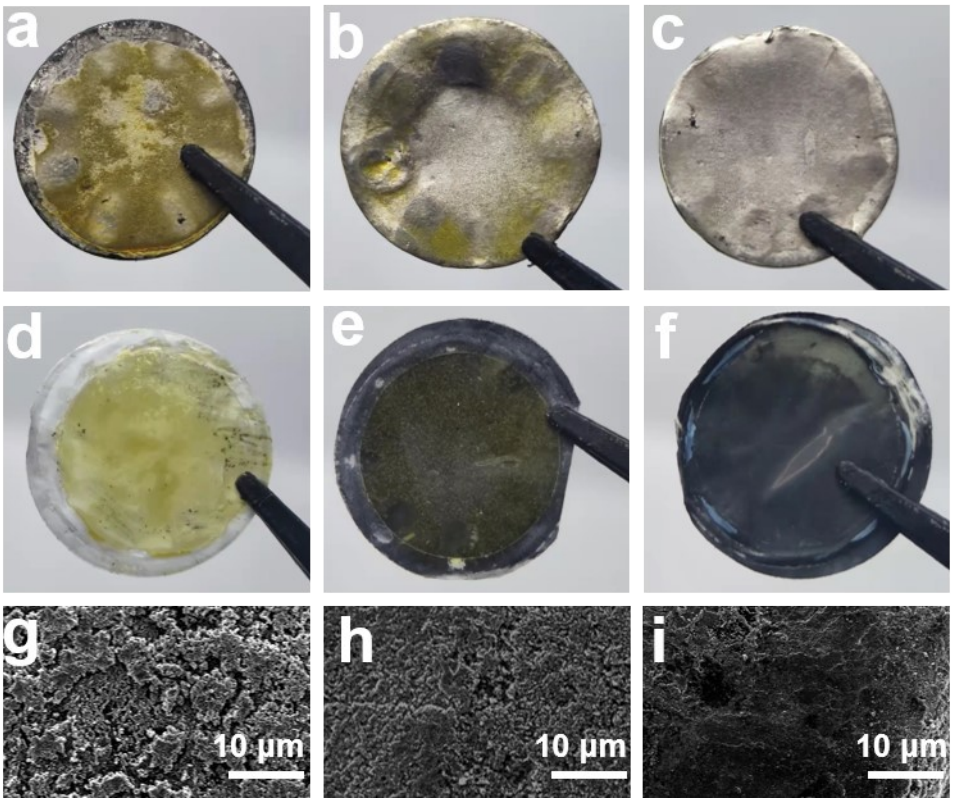

Fig. S12 Digital images of Li-S batteries after 200 cycles at 0.2 C when paired with (a) PP, (b) NG, (c) NbN@NG separators and (d-f) corresponding Li-metal anodes. (g-i) SEM images of corresponding Li-metal anodes.

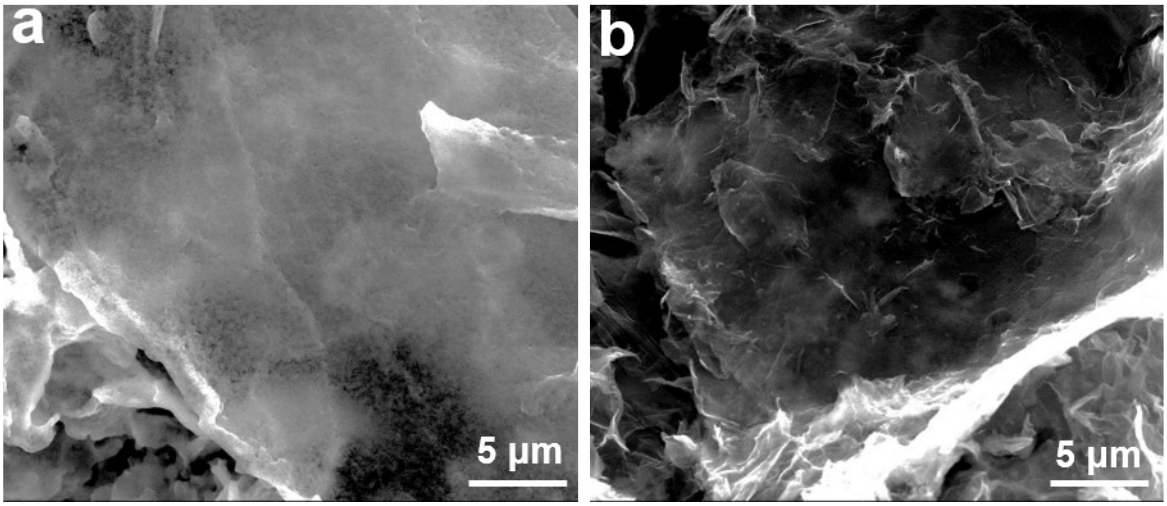

Fig. S13 FESEM images of the (a) NG and (b) NbN@NG modified separators after 200 cycles at 0.2 C.

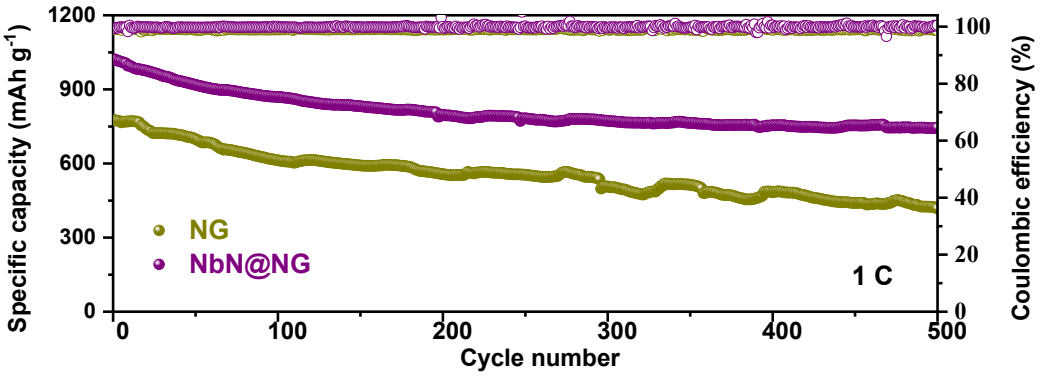

Fig. S14 Long cycle performance test for the batteries at 1C.

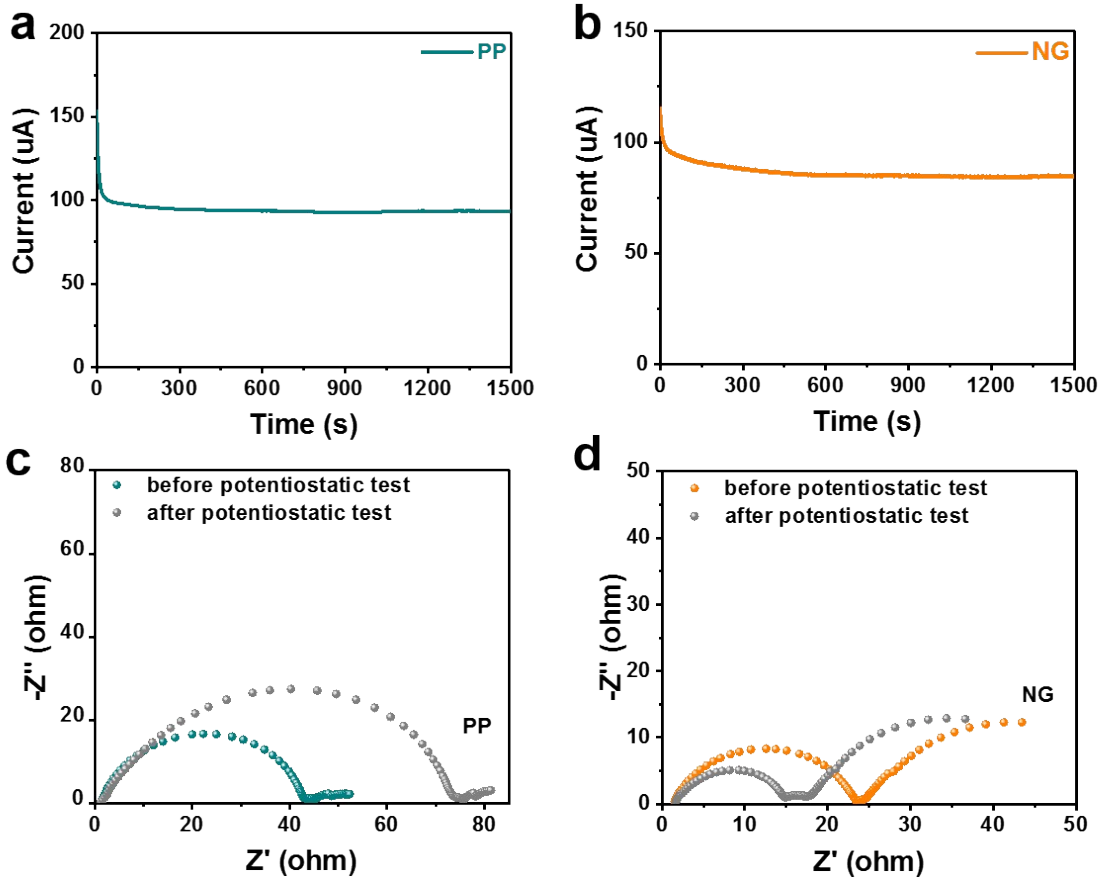

Fig. S15 I-t curves and the corresponding EIS plots of the batteries with separators of (a, c) PP and (b, d) NG.

Fig. S16 Digital photographs of an in-situ Raman test configuration.

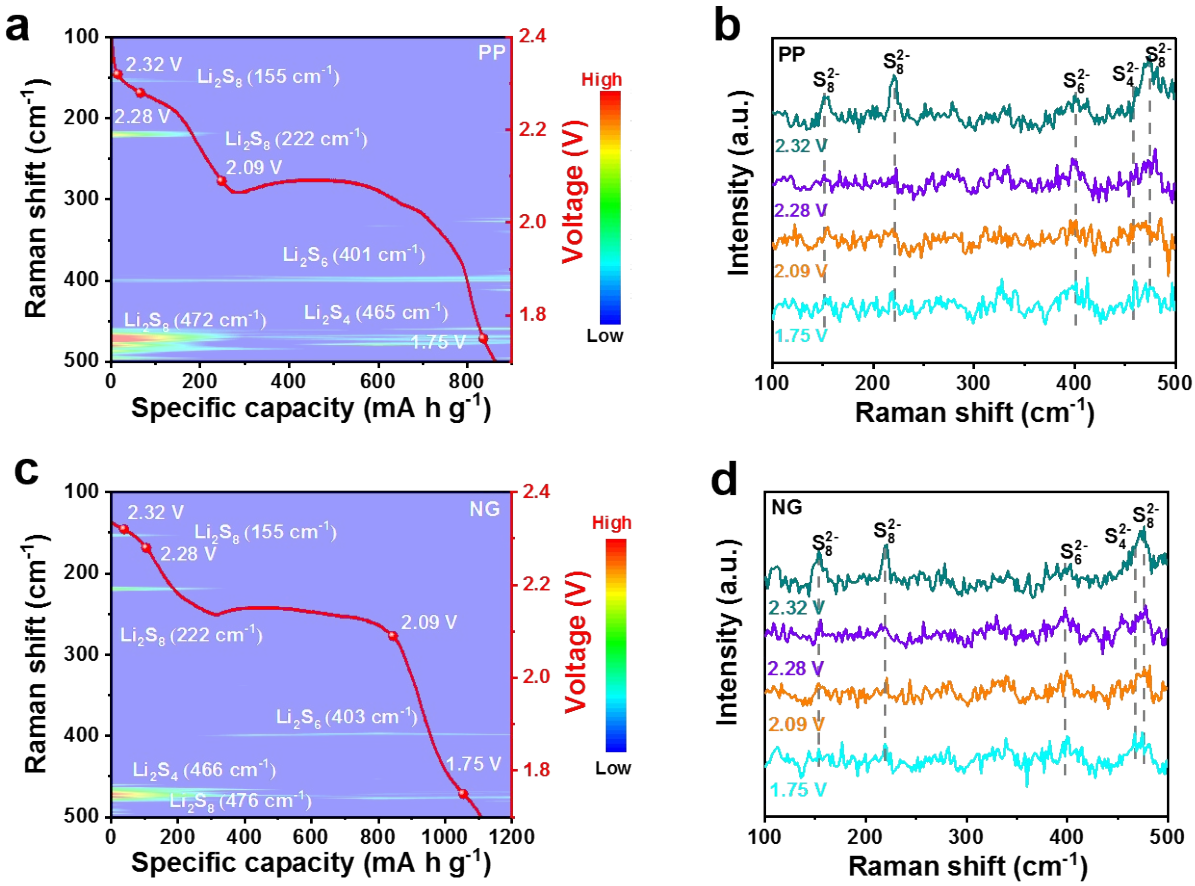

Fig. S17 (a, c) In situ time-resolved Raman spectra and (b, d) selected Raman spectroscopy of Li-S cells based on PP and NG modified separators during the discharging processes.

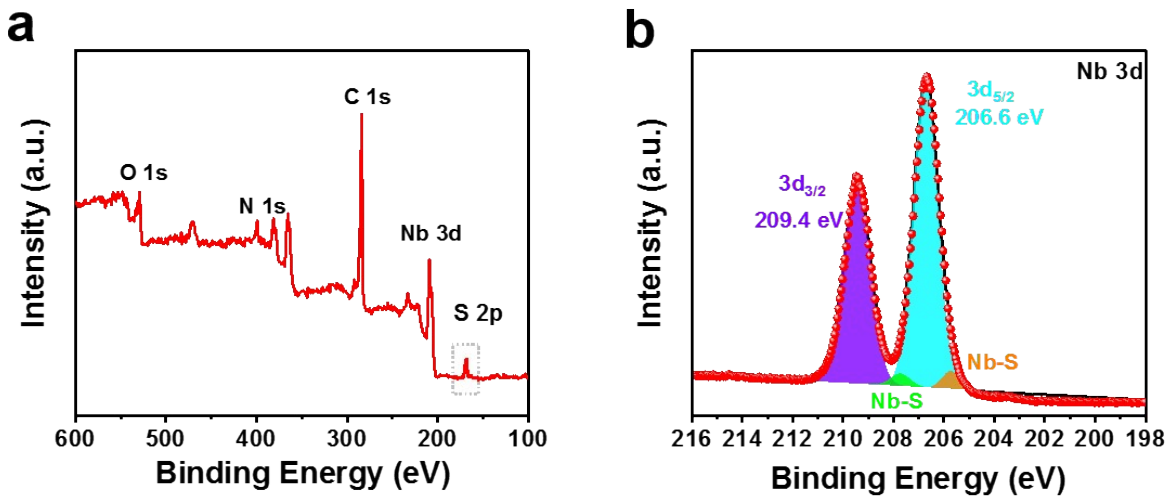

Fig. S18 (a) XPS spectrum of the NbN@NG + Li_2S_6 sample. (b) The corresponding Nb 3d XPS spectrum after LiPSs adsorption test.

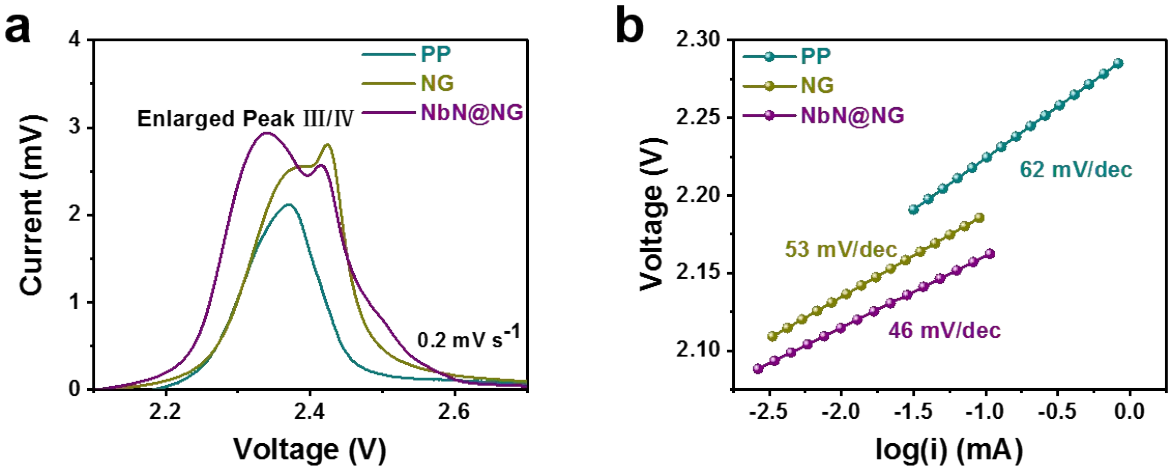

Fig. S19 LSV profiles of an enlarged view in (a) peak III and peak IV of Li-S batteries with different separators. (b) Tafel plots calculated from reduction peak II and oxidation peak III.

Table S1. Summary of electrochemical parameters of different separators

Modified separator	PP	NG	NbN@NG
D_{Li+} at peak 1 ($cm^2\ s^{-1}$)	6.779×10^{-8}	1.211×10^{-7}	2.227×10^{-7}
D_{Li+} at peak 2 ($cm^2\ s^{-1}$)	1.444×10^{-8}	3.115×10^{-8}	5.538×10^{-8}
D_{Li+} at peak 3 ($cm^2\ s^{-1}$)	1.504×10^{-8}	2.072×10^{-8}	2.984×10^{-8}
Li^+ conductivity ($mS\ cm^{-1}$)	0.869	0.374	0.765
Li^+ transfer number	0.623	0.747	0.876

Table S2. EIS fitting results of Li-S batteries paired with different separators before cycling

Modified separator	PP	NG	NbN@NG
R_e (Ω)	3.61	6.47	3.38
Rct (Ω)	72.64	62.96	30.57

Table S3. EIS fitting results of Li-S batteries paired with different separators after cycling

Modified separator	PP	NbN	NbN@NG
R_e (Ω)	7.55	7.38	4.63
Rct (Ω)	50.88	45.61	22.15
Rs (Ω)	13.77	9.02	2.17

Table S4. Electrochemical performances of this work compared with previous works involving different separators in recently reported literature.

Modifid separator	S loading (mg cm^{-2})	Coating loading (mg cm^{-2})	Rate capacity (mA h g^{-1})	Capacity decay rate/cycle number/ C rate	Ref.
TiN	1.3	1	782 (2C)	0.085%/300/2C	1
VN	1.6	1.52	760 (2C)	0.077%/800/1C	2
CNT/MoP_2	1.2	0.58	1223 (0.2C)	0.152%/100/0.2C	3
NbN	2.0	0.2	800 (1C)	0.08%/300/1C	4
VSe_2 NC@NG	--	0.07-0.11	6000 (8C)	0.052%/550/2C	5
Co_9S_8/CoO	1.0	0.3	536 (5C)	0.014%/300/1C	6
CoNi@MPC	1.0-1.5	--	665.3 (4C)	0.087%/500/4C	7
MoS_2	1.6	--	550 (C)	0.083%/600/0.5C	8
Sb_2S_3/CNT	1.0	--	770 (2C)	0.05%/200/2C	9
Co/mSiO_2-NCNTs	1.15	0.25	552 (5C)	0.09%/2501C	10
NbN@NG	**1.3-1.6**	**0.25-0.28**	**819 (4C)**	**0.036%/500/2C**	**This work**

References

1 B. Qi, X. Zhao, S. Wang, K. Chen, Y. Wei, G. Chen, Y. Gao, D. Zhang, Z. Sun and F. Li, *J. Mater. Chem. A*, 2018, **6**, 14359-14366.

2 Y. Song, S. Zhao, Y. Chen, J. Cai, J. Li, Q. Yang, J. Sun and Z. Liu, *ACS Appl. Mater. Interfaces*, 2019, **11**, 5687-5694.

3 Y. Luo, N. Luo, W. Kong, H. Wu, K. Wang, S. Fan, W. Duan and J. Wang, *Small*, 2018, **14**, 1702853.

4 S. Kim, W. Lim, A. Cho, J. Jeong, C. Jo, D. Kang, S. M. Han, J. W. Han and J. Lee, *ACS Applied Energy Mater.*, 2020, **3**, 2643-2652.

5 W. Tian, B. Xi, Y. Gu, Q. Fu, Z. Feng, J. Feng and S. Xiong, *Nano Res.*, 2020, **13**, 2673-2682.

6 N. Wang, B. Chen, K. Qin, E. Liu, C. Shi, C. He and N. Zhao, *Nano Energy*, 2019, **60**, 332-339.

7 R. Luo, Z. Zhang, J. Zhang, B. Xi, F. Tian, W. Chen, J. Feng and S. Xiong, *Small*, 2021, **17**, 2100414.

8 Z. A. Ghazi, X. He, A. M. Khattak, N. A. Khan, B. Liang, A. Iqbal, J. Wang, H. Sin, L. Li and Z. Tang, *Adv. Mater.*, 2017, **29**, 1606817.

9 S. Yao, J. Cui, J. Q. Huang, Z. Lu, Y. Deng, W. G. Chong, J. Wu, M. Ihsan Ul Haq, F. Ciucci and J. K. Kim, *Adv. Energy Mater.*, 2018, **8**, 1800710.

10 D. Fang, Y. Wang, X. Liu, J. Yu, C. Qian, S. Chen, X. Wang and S. Zhang, *ACS Nano*, 2019.